

ONE-LOOP RUNNING OF DIMENSION-SIX
HIGGS-NEUTRINO OPERATORS AND
IMPLICATIONS OF A LARGE NEUTRINO DIPOLE MOMENT

Mikael Chala^a and Arsenii Titov^b

^a*CAFPE and Departamento de Física Teórica y del Cosmos, Universidad de Granada,
Campus de Fuentenueva, E-18071 Granada, Spain*

^b*Dipartimento di Fisica e Astronomia “G. Galilei”, Università degli Studi di Padova
and INFN, Sezione di Padova, Via Francesco Marzolo 8, I-35131 Padova, Italy*

Abstract

We compute the one-loop running of the dimension-six CP-even Higgs operators in the Standard Model effective field theory involving the right-handed component of the would-be Dirac neutrinos. Then, on the basis of naturalness arguments, for some operators we obtain bounds that surpass direct constraints by orders of magnitude. We also discuss the implications of a large Dirac neutrino magnetic dipole moment. In particular, we demonstrate that a neutrino magnetic moment explaining the recent XENON1T excess induces Higgs and Z invisible decays with branching ratios in the range $[10^{-18}, 10^{-12}]$. These numbers are unfortunately beyond the reach of current and near future facilities.

1 Introduction

The Standard Model (SM) effective field theory (EFT) [1, 2] is the right tool to describe physics above the electroweak (EW) scale. Its use has been boosted in the last years [3] in light of the null results (modulo a few non-conclusive anomalies [4–6]) in the search for new physics at different facilities, and in particular at the LHC. The necessity of using this framework across a wide range of energies has also triggered the computation of the one-loop renormalisation group equations (RGEs) for the dimension-six operators [7–13]. The RGEs in the theory valid at energies below the EW scale where the top quark, the Higgs and the W and Z gauge bosons are integrated out, usually referred to as LEFT, are also known [14]; as well as the matching between the SMEFT and the LEFT at up to one loop [15, 16]. Likewise, the desire of connecting the SMEFT to ultraviolet (UV) models has stimulated different works on the matching procedure [17–26]; including more recently the first basis of dimension-six operators suitable for off-shell integration [27].

All the aforementioned works assume that neutrinos are Majorana fermions. Notwithstanding the good motivation for this option—in particular lepton number (LN) is only an approximate symmetry of the renormalisable SM Lagrangian—it should not be forgotten that there is absolutely no experimental evidence that neutrinos are not just Dirac particles as all the other SM fermions. There is even theoretical support for this ¹. However, the SMEFT that includes the right-handed (RH) neutrinos N , also known as NSMEFT [31, 32], has been explored to a smaller extent; see Refs. [33–41] for phenomenological works. The off-shell basis of the NSMEFT has only recently been worked out in Ref. [42], where the NLEFT and the tree-level matching between the two EFTs are also presented. More importantly, only the gauge dependence of the RGEs of only very small set of operators are known [43, 44].

Our aim in this paper is to compute the one-loop RGE matrix of the NSMEFT Higgs operators in full detail and to discuss the phenomenological implications, particularly in light of the recent XENON1T observation of an excess of low-energy electron recoil events [6].

The article is organised as follows. In section 2 we introduce the NSMEFT and discuss the generic structure of the RGEs. In section 3 we thoroughly discuss the matching of the UV divergences onto the EFT. We obtain the corresponding counterterms and derive our main result, namely the 5×5 anomalous dimension matrix to one loop, in section 4. In section 5 we discuss some phenomenological implications. In particular, the aforementioned XENON1T anomaly might point out to a large neutrino magnetic dipole moment; we demonstrate that it leads to irreducible Higgs and Z invisible decays and we quantify their magnitude. We conclude in section 6, while Appendix A is dedicated to

¹For example, Refs. [28, 29] show that the SM with only 3 Majorana neutrinos does satisfy the sharpened version of the weak gravity conjecture by Ooguri and Vafa [30], presumably implying that such SM cannot be consistently embedded into a quantum theory of gravity.

different cross-checks of our computation.

2 The lepton number conserving Standard Model effective field theory

We denote by e, u and d the RH leptons and quarks; and by L and Q the left-handed (LH) counterparts. The gluon and the EW gauge bosons are named by G and W, B , respectively. We represent the Higgs doublet by $H = (H^+, H_0)^T$, and $\tilde{H} = i\sigma_2 H^*$, with $\sigma_I, I = 1, 2, 3$, being the Pauli matrices.

Our conventions for the covariant derivative and for the field strength tensors are

$$D_\mu = \partial_\mu - ig_1 Y B_\mu - ig_2 \frac{\sigma^I}{2} W_\mu^I - ig_s \frac{\lambda^A}{2} G_\mu^A, \quad (2.1)$$

and

$$B_{\mu\nu} = \partial_\mu B_\nu - \partial_\nu B_\mu, \quad (2.2)$$

$$W_{\mu\nu}^I = \partial_\mu W_\nu^I - \partial_\nu W_\mu^I + g_2 \epsilon^{IJK} W_\mu^J W_\nu^K, \quad (2.3)$$

$$G_{\mu\nu}^A = \partial_\mu G_\nu^A - \partial_\nu G_\mu^A + g_s f^{ABC} G_\mu^B G_\nu^C, \quad (2.4)$$

where Y stands for the hypercharge and $\lambda^A, A = 1, \dots, 8$, are the Gell-Mann matrices; while ϵ^{IJK} and f^{ABC} represent the $SU(2)_L$ and $SU(3)_c$ structure constants.

We denote by N the RH component of the neutrino. The renormalisable Lagrangian of the NSMEFT reads

$$\begin{aligned} \mathcal{L}_4 = & -\frac{1}{4} G_{\mu\nu}^A G^{A\mu\nu} - \frac{1}{4} W_{\mu\nu}^I W^{I\mu\nu} - \frac{1}{4} B_{\mu\nu} B^{\mu\nu} \\ & + (D_\mu H)^\dagger (D^\mu H) + \mu_H^2 H^\dagger H - \frac{1}{2} \lambda_H (H^\dagger H)^2 \\ & + i (\bar{Q} \not{D} Q + \bar{u} \not{D} u + \bar{d} \not{D} d + \bar{L} \not{D} L + \bar{e} \not{D} e + \bar{N} \not{D} N) \\ & - \left[\bar{Q} Y_d H d + \bar{Q} Y_u \tilde{H} u + \bar{L} Y_e H e + \bar{L} Y_N \tilde{H} N + \text{h.c.} \right]. \end{aligned} \quad (2.5)$$

The dimension-six interactions,

$$\mathcal{L}_6 = \frac{1}{\Lambda^2} \sum_i \alpha_i \mathcal{O}_i, \quad (2.6)$$

can be expressed in terms of a basis of effective operators. We choose the latter to consist of the SMEFT operators in Ref. [2] (which do not contain N) plus those in Tabs. 1 and 2. The α_i represent Wilson coefficients. As we enforce LN conservation, there are no dimension-five operators.

0-Higgs	1-Higgs	2-Higgs
$\mathcal{O}_{DN}^1 = \bar{N}\partial^2\phi N$	$\mathcal{O}_{NB} = \bar{L}\sigma^{\mu\nu}N\tilde{H}B_{\mu\nu}$, $\mathcal{O}_{NW} = \bar{L}\sigma^{\mu\nu}N\sigma_I\tilde{H}W_{\mu\nu}^I$	$\mathcal{O}_{HN} = \bar{N}\gamma^\mu N(H^\dagger iD_\mu H)$
$\mathcal{O}_{DN}^2 = i\tilde{B}_{\mu\nu}(\bar{N}\gamma^\mu\partial^\nu N)$	$\mathcal{O}_{LN}^1 = \bar{L}ND^2\tilde{H}$, $\mathcal{O}_{LN}^2 = \bar{L}\partial_\mu ND^\mu\tilde{H}$	$\mathcal{O}_{NN}^2 = \bar{N}i\phi N(H^\dagger H)$
$\mathcal{O}_{DN}^3 = \partial^\nu B_{\mu\nu}(\bar{N}\gamma^\mu N)$	$\mathcal{O}_{LN}^3 = i\bar{L}\sigma^{\mu\nu}\partial_\mu ND_\nu\tilde{H}$, $\mathcal{O}_{LN}^4 = \bar{L}(\partial^2 N)\tilde{H}$	$\mathcal{O}_{HNe} = \bar{N}\gamma^\mu e(\tilde{H}^\dagger iD_\mu H)$
3-Higgs: $\mathcal{O}_{LNH} = \bar{L}\tilde{H}N(H^\dagger H)$		

Table 1: *Relevant CP-even bosonic operators. The h.c. is implied when needed. For example, $\mathcal{O}_{DN}^1 = \bar{N}\partial^2\phi N + h.c.$ So all Wilson coefficients are hermitian. The CP-odd operators include $iB_{\mu\nu}(\bar{N}\gamma^\mu\partial^\nu N)$, $i\mathcal{O}_{NB}$, $i\mathcal{O}_{NW}$, $i\mathcal{O}_{LN}^{1,2,3,4}$, $i\mathcal{O}_{LNH}$, $i\mathcal{O}_{HN}$ and $i\mathcal{O}_{HNe}$ [42].*

RRRR	$\mathcal{O}_{NN} = (\bar{N}\gamma_\mu N)(\bar{N}\gamma^\mu N)$	
	$\mathcal{O}_{eN} = (\bar{e}\gamma_\mu e)(\bar{N}\gamma^\mu N)$	$\mathcal{O}_{uN} = (\bar{u}\gamma_\mu u)(\bar{N}\gamma^\mu N)$
	$\mathcal{O}_{dN} = (\bar{d}\gamma_\mu d)(\bar{N}\gamma^\mu N)$	$\mathcal{O}_{duNe} = (\bar{d}\gamma_\mu u)(\bar{N}\gamma^\mu e)$
LLRR	$\mathcal{O}_{LN} = (\bar{L}\gamma_\mu L)(\bar{N}\gamma^\mu N)$	$\mathcal{O}_{QN} = (\bar{Q}\gamma_\mu Q)(\bar{N}\gamma^\mu N)$
LRLR	$\mathcal{O}_{LNLe} = (\bar{L}N)\epsilon(\bar{L}e)$	$\mathcal{O}_{LNQd} = (\bar{L}N)\epsilon(\bar{Q}d)$
	$\mathcal{O}_{LdQN} = (\bar{L}d)\epsilon(\bar{Q}N)$	
LRRL	$\mathcal{O}_{QuNL} = (\bar{Q}u)(\bar{N}L)$	

Table 2: *CP-even four-fermion operators. The CP-odd ones carry an extra imaginary unit.*

In this work we are only interested in the CP-even sector of the theory. Therefore, in good approximation we can assume that $Y_u = \text{diag}(y_u, y_c, y_t)$, while $Y_d = \text{diag}(y_d, y_s, y_b)$ and $Y_e = \text{diag}(y_e, y_\mu, y_\tau)$ without loss of generality.

In good approximation we can also assume that there is no huge fine-tuning between the operators entering into the expression for the neutrino mass, $m_\nu \sim Y_N v - \alpha_{LNH} v^3/\Lambda^2$, so in particular Y_N can be neglected². This also implies that lepton flavour is conserved in \mathcal{L}_4 . For simplicity we focus on the regime in which lepton flavour is also conserved in the N sector of \mathcal{L}_6 . As a consequence, the three lepton families factorise (in particular they evolve independently under the RGEs). We can therefore ignore flavour indices for clarity.

The operators in grey in Tabs. 1 and 2 are redundant when evaluated on shell; the

²Even if, as we show below, α_{LNH} is generated radiatively and therefore $Y_N \sim g^2 v^2/(16\pi^2 \Lambda^2)$ to keep m_ν small, Y_N is of order $\lesssim 10^{-4}$ for $\Lambda = 1$ TeV, and hence much smaller than even the muon Yukawa.

redundancies due to algebraic or Fierz identities or ensuing from integration by parts have been removed. We refer to this basis as *off-shell* or *Green* basis; see Ref. [27] for a Green basis of the sector with no N .

The relevant equations of motion of \mathcal{L}_4 for the fermions read:

$$i\cancel{D}L = Y_e H e + Y_N \tilde{H} N, \quad (2.7)$$

$$i\cancel{D}N = Y_N^\dagger \tilde{H}^\dagger L, \quad (2.8)$$

$$i\cancel{D}e = Y_e^\dagger H^\dagger L, \quad (2.9)$$

$$i\cancel{D}Q = Y_u \tilde{H} u + Y_d H d, \quad (2.10)$$

$$i\cancel{D}u = Y_u^\dagger \tilde{H}^\dagger Q, \quad (2.11)$$

$$i\cancel{D}d = Y_d^\dagger H^\dagger Q; \quad (2.12)$$

while for the bosons we have instead:

$$(D^2 \tilde{H})^i = \mu_H^2 \tilde{H}^i - \lambda_H (H^\dagger H) \tilde{H}^i - \epsilon_{ij} \bar{Q}^j Y_d d - \bar{u} Y_u^\dagger Q^i - \epsilon_{ij} \bar{L}^j Y_e e - \bar{N} Y_N L^i, \quad (2.13)$$

$$\partial^\nu B_{\nu\mu} = -\frac{g_1}{2} (iH^\dagger D_\mu H + \text{h.c.}) - g_1 Y^f \bar{f} \gamma_\mu f, \quad (2.14)$$

$$D^\nu W_{\nu\mu}^I = -\frac{g_2}{2} (H^\dagger iD_\mu^I H - iD_\mu^I H^\dagger H + \bar{L} \gamma_\mu \sigma^I L + \bar{Q} \gamma_\mu \sigma^I Q), \quad (2.15)$$

$$D^\nu G_{\nu\mu}^A = -\frac{g_s}{2} (\bar{Q} \gamma_\mu \lambda^A Q + \bar{u} \gamma_\mu \lambda^A u + \bar{d} \gamma_\mu \lambda^A d); \quad (2.16)$$

where f runs over all fermions. As a consequence, the following relations hold on shell for the operators in grey in Tab. 1:

$$\mathcal{O}_{DN}^1 = 0 + \dots, \quad (2.17)$$

$$\mathcal{O}_{DN}^2 = -\frac{g_1}{2} \mathcal{O}_{HN} + \dots, \quad (2.18)$$

$$\mathcal{O}_{DN}^3 = -\mathcal{O}_{DN}^2 + \dots, \quad (2.19)$$

$$\mathcal{O}_{LN}^1 = \left(\mu_H^2 \bar{L} \tilde{H} N + \text{h.c.} \right) - \lambda_H \mathcal{O}_{LNH} + \dots, \quad (2.20)$$

$$\mathcal{O}_{LN}^2 = -\frac{1}{2} Y_e \mathcal{O}_{HN} - \left(\frac{\mu_H^2}{2} \bar{L} \tilde{H} N + \text{h.c.} \right) + \frac{\lambda_H}{2} \mathcal{O}_{LNH} - \frac{g_1}{8} \mathcal{O}_{NB} + \frac{g_2}{8} \mathcal{O}_{NW} + \dots, \quad (2.21)$$

$$\mathcal{O}_{LN}^3 = -\mathcal{O}_{LN}^2 + \dots, \quad (2.22)$$

$$\mathcal{O}_{LN}^4 = 0 + \dots, \quad (2.23)$$

$$\mathcal{O}_{NN}^2 = 0 + \dots. \quad (2.24)$$

The ellipses represent Y_N suppressed operators (which might include CP-odd ones) and/or four-fermions, which we ignore ³.

³ While loops of bosonic operators can generate contact interactions, the latter cannot contribute back to bosonic operators via equations of motion and they can therefore be consistently ignored.

Under RG running the Wilson coefficients evolve as

$$\vec{\beta} \equiv 16\pi^2\mu\frac{d\vec{\alpha}}{d\mu} = \gamma\vec{\alpha}, \quad (2.25)$$

where $\vec{\alpha}$ is a vector that collects the Wilson coefficients of the EFT basis and γ is the so-called *anomalous dimension matrix*.

Given the previous discussion, we can anticipate the global structure of γ :

$$\gamma = \begin{pmatrix} \boxed{\gamma^{\text{SMEFT}}} & & & & & & \\ & \times & \times & 0 & 0 & 0 & \\ & \times & \times & 0 & 0 & 0 & \\ & \times & \times & \times & \mathcal{O}(Y_e) & \mathcal{O}(Y_e) & \\ & \times & \times & \mathcal{O}(Y_e) & \times & \mathcal{O}(Y_e) & \\ & \times & \times & \mathcal{O}(Y_e) & \mathcal{O}(Y_e) & \times & \end{pmatrix} \begin{matrix} \alpha_{NB} \\ \alpha_{NW} \\ \alpha_{HN} \\ \alpha_{HNe} \\ \alpha_{LNH} \end{matrix}, \quad (2.26)$$

where γ^{SMEFT} stands for the 59×59 matrix (ignoring flavour indices) accounting for the RG evolution of purely SMEFT operators [10–12]. Because we neglect Y_N , N does not interact with any other field at the renormalisable level. Therefore, operators involving N cannot renormalise purely SMEFT operators, and vice versa. This explains the block-diagonal form of the matrix in Eq. (2.26).

The almost diagonal structure in the block of $\{\mathcal{O}_{HN}, \mathcal{O}_{HNe}, \mathcal{O}_{LNH}\}$, only broken by Y_e , can be explained as follows. Let us define the symmetries $\mathbb{L}_e : e \rightarrow \exp(i\theta_e)e$, $\mathbb{L}_N : N \rightarrow \exp(i\theta_N)N$ and $\mathbb{L}_H : H \rightarrow \exp(i\theta_H)H$. In the limit $Y_e \rightarrow 0$, \mathcal{L}_4 is completely invariant under the simultaneous action of \mathbb{L}_e , \mathbb{L}_N and \mathbb{L}_H , therefore dimension-four loop corrections to dimension-six operators cannot modify the e , N and Higgs numbers; not even by equations of motion. However, \mathcal{O}_{HN} , \mathcal{O}_{HNe} and \mathcal{O}_{LNH} differ among themselves in at least one of these quantum numbers.

The main result of this paper is the exact one-loop expression for the 5×5 lower block in γ , the calculation of which we discuss in detail in the next sections.

3 Computation of the divergences

We use the background field method. Each of the gauge bosons is thus split into a background field and a quantum fluctuation that can only appear in loops in Feynman diagrams. We work in the Feynman gauge. The latter is fixed only with respect to the quantum fluctuations, therefore even non-physical quantities such as counterterms are manifestly gauge invariant. Consequently, to order $\mathcal{O}(1/\Lambda^2)$, any one-loop amplitude (and the divergences themselves) can be unambiguously mapped onto the EFT basis of Tab. 1. Note also that because this Green basis contains operators related by field redefinitions, we can restrict our calculations to (off-shell) one-particle-irreducible amplitudes.

Let us first consider the amplitude for $\overline{N}(p_1)N(p_2) \rightarrow B(p_3)$. Hereafter we work in dimensional regularisation with space-time dimension $d = 4 - 2\epsilon$ and absorb $1/\Lambda^2$ in the Wilson coefficients in the expressions for amplitudes. Using **FeynArts** [45] together with **FormCalc** [46] we obtain the following one-loop divergence to order $\mathcal{O}(p^2)$:

$$i\mathcal{M}_{\text{loop}} = \frac{i}{48\pi^2\epsilon} g_1 \alpha_{HN} \overline{v}_1 \left(p_3^2 \gamma^\mu - p_3^\mu \not{p}_3 \right) P_R u_2 \epsilon_\mu^*. \quad (3.1)$$

Here and in what follows $v_1 \equiv v(p_1)$, $u_2 \equiv u(p_2)$ and $\epsilon_\mu^* \equiv \epsilon_\mu^*(p_3)$. The most generic divergence in the EFT depends only on \mathcal{O}_{DN}^2 and \mathcal{O}_{DN}^3 . It reads

$$i\mathcal{M}_{\text{div}} = i\overline{v}_1 \left[\tilde{\alpha}_{DN}^3 \left(p_3^\mu \not{p}_3 - p_3^2 \gamma^\mu \right) + 2\tilde{\alpha}_{DN}^2 \left(\gamma^\mu p_2 p_3 - \gamma^\mu \not{p}_3 \not{p}_2 + p_3^\mu \not{p}_2 - p_2^\mu \not{p}_3 \right) \right] P_R u_2 \epsilon_\mu^*. \quad (3.2)$$

Upon equating $\mathcal{M}_{\text{loop}}$ and \mathcal{M}_{div} , we obtain:

$$\tilde{\alpha}_{DN}^2 = 0, \quad (3.3)$$

$$\tilde{\alpha}_{DN}^3 = -\frac{1}{48\pi^2\epsilon} g_1 \alpha_{HN}. \quad (3.4)$$

For the amplitude for $\overline{\nu}_L(p_1)N(p_2) \rightarrow H_0(p_3)$ at $\mathcal{O}(p^2)$ we obtain:

$$i\mathcal{M}_{\text{loop}} = \frac{i}{32\pi^2\epsilon} \overline{v}_1 \left[(3g_1\alpha_{NB} - 9g_2\alpha_{NW} + 2Y_e\alpha_{HNe}) p_1^2 + Y_e\alpha_{HNe} \not{p}_1 \not{p}_2 \right] P_R u_2, \quad (3.5)$$

and

$$i\mathcal{M}_{\text{div}} = i\overline{v}_1 \left[\tilde{\alpha}_{LN}^1 p_1^2 + (\tilde{\alpha}_{LN}^1 - \tilde{\alpha}_{LN}^2 + \tilde{\alpha}_{LN}^4) p_2^2 + (2\tilde{\alpha}_{LN}^1 - \tilde{\alpha}_{LN}^2 + \tilde{\alpha}_{LN}^3) p_1 p_2 - \tilde{\alpha}_{LN}^3 \not{p}_1 \not{p}_2 \right] P_R u_2, \quad (3.6)$$

which implies

$$\tilde{\alpha}_{LN}^1 = \frac{1}{32\pi^2\epsilon} (3g_1\alpha_{NB} - 9g_2\alpha_{NW} + 2Y_e\alpha_{HNe}), \quad (3.7)$$

$$\tilde{\alpha}_{LN}^2 = \frac{3}{32\pi^2\epsilon} (2g_1\alpha_{NB} - 6g_2\alpha_{NW} + Y_e\alpha_{HNe}), \quad (3.8)$$

$$\tilde{\alpha}_{LN}^3 = -\frac{1}{32\pi^2\epsilon} Y_e\alpha_{HNe}, \quad (3.9)$$

$$\tilde{\alpha}_{LN}^4 = \frac{1}{32\pi^2\epsilon} (3g_1\alpha_{NB} - 9g_2\alpha_{NW} + Y_e\alpha_{HNe}). \quad (3.10)$$

For the amplitude for $\overline{\nu}_L(p_1)N(p_2) \rightarrow B(p_3)H_0(p_4)$ at linear order in the external momenta we get:

$$i\mathcal{M}_{\text{loop}} = \frac{i}{64\pi^2\epsilon} \overline{v}_1 \left\{ 2 (3g_1^2\alpha_{NB} - 9g_1g_2\alpha_{NW} + 2g_1Y_e\alpha_{HNe}) p_1^\mu \right.$$

$$\begin{aligned}
& + 2 \left[(3g_2^2 - 2g_1^2 + 4Y_e^2) \alpha_{NB} + 9g_1g_2\alpha_{NW} \right] p_3^\mu + g_1 Y_e \alpha_{HNe} \gamma^\mu \not{p}_2 \\
& + \left[(g_1^2 - 6g_2^2 - 8Y_e^2) \alpha_{NB} - 9g_1g_2\alpha_{NW} - 2g_1 Y_e \alpha_{HNe} \right] \gamma^\mu \not{p}_3 \left. \right\} P_R u_2 \epsilon_\mu^*, \quad (3.11)
\end{aligned}$$

as well as

$$\begin{aligned}
i\mathcal{M}_{\text{div}} = & ig_1 \bar{v}_1 \left[\tilde{\alpha}_{LN}^1 p_1^\mu + \left(\tilde{\alpha}_{LN}^1 - \frac{1}{2} \tilde{\alpha}_{LN}^2 + \frac{1}{2} \tilde{\alpha}_{LN}^3 \right) p_2^\mu + \left(2 \frac{\tilde{\alpha}_{NB}}{g_1} - \frac{1}{2} \tilde{\alpha}_{LN}^1 \right) p_3^\mu \right. \\
& \left. - \frac{1}{2} \tilde{\alpha}_{LN}^3 \gamma^\mu \not{p}_2 - 2 \frac{\tilde{\alpha}_{NB}}{g_1} \gamma^\mu \not{p}_3 \right] P_R u_2 \epsilon_\mu^*. \quad (3.12)
\end{aligned}$$

Upon equating both quantities, we obtain the same values of $\tilde{\alpha}_{LN}^1$, $\tilde{\alpha}_{LN}^2$ and $\tilde{\alpha}_{LN}^3$ as before (what provides a strong cross-check of the computation), as well as

$$\tilde{\alpha}_{NB} = \frac{1}{128\pi^2\epsilon} \left[(6g_2^2 - g_1^2 + 8Y_e^2) \alpha_{NB} + 9g_1g_2\alpha_{NW} + 2g_1 Y_e \alpha_{HNe} \right]. \quad (3.13)$$

The divergences at one loop and in the EFT for $\bar{e}_L(p_1)N(p_2) \rightarrow W^3(p_3)H^+(p_4)$ at $\mathcal{O}(p)$ read respectively:

$$\begin{aligned}
i\mathcal{M}_{\text{loop}} = & \frac{i}{64\pi^2\epsilon} \bar{v}_1 \left\{ 2g_2 (9g_2\alpha_{NW} - 3g_1\alpha_{NB} - 2Y_e\alpha_{HNe}) p_1^\mu \right. \\
& + 2 \left[3g_1g_2\alpha_{NB} + (g_1^2 - 6g_2^2 - 4Y_e^2) \alpha_{NW} \right] p_3^\mu \\
& - g_2 Y_e \alpha_{HNe} \gamma^\mu \not{p}_2 \\
& \left. - \left[3g_1g_2\alpha_{NB} + (2g_1^2 - 3g_2^2 - 8Y_e^2) \alpha_{NW} - 2g_2 Y_e \alpha_{HNe} \right] \gamma^\mu \not{p}_3 \right\} P_R u_2 \epsilon_\mu^*, \quad (3.14)
\end{aligned}$$

and

$$\begin{aligned}
i\mathcal{M}_{\text{div}} = & ig_2 \bar{v}_1 \left[-\tilde{\alpha}_{LN}^1 p_1^\mu - \left(\tilde{\alpha}_{LN}^1 - \frac{1}{2} \tilde{\alpha}_{LN}^2 + \frac{1}{2} \tilde{\alpha}_{LN}^3 \right) p_2^\mu + \left(2 \frac{\tilde{\alpha}_{NW}}{g_2} + \frac{1}{2} \tilde{\alpha}_{LN}^1 \right) p_3^\mu \right. \\
& \left. + \frac{1}{2} \tilde{\alpha}_{LN}^3 \gamma^\mu \not{p}_2 - 2 \frac{\tilde{\alpha}_{NW}}{g_2} \gamma^\mu \not{p}_3 \right] P_R u_2 \epsilon_\mu^*. \quad (3.15)
\end{aligned}$$

This cross-checks again $\tilde{\alpha}_{LN}^1$, $\tilde{\alpha}_{LN}^2$ and $\tilde{\alpha}_{LN}^3$ and also leads to

$$\tilde{\alpha}_{NW} = \frac{1}{128\pi^2\epsilon} \left[3g_1g_2\alpha_{NB} + (2g_1^2 - 3g_2^2 - 8Y_e^2) \alpha_{NW} - 2g_2 Y_e \alpha_{HNe} \right]. \quad (3.16)$$

For $\bar{N}(p_1)N(p_2) \rightarrow H_0^*(p_3)H_0(p_4)$ to $\mathcal{O}(p)$ in the external momenta, we have:

$$i\mathcal{M}_{\text{loop}} = \frac{i}{32\pi^2\epsilon} (g_1^2 + 3g_2^2) \alpha_{HN} \bar{v}_1 \left(\not{p}_1 + \not{p}_2 - 2\not{p}_3 \right) u_2, \quad (3.17)$$

and

$$i\mathcal{M}_{\text{div}} = i\bar{v}_1 \left[(\tilde{\alpha}_{NN}^2 - \tilde{\alpha}_{HN}) \not{p}_1 - (\tilde{\alpha}_{NN}^2 + \tilde{\alpha}_{HN}) \not{p}_2 + 2\tilde{\alpha}_{HN} \not{p}_3 \right] P_R u_2. \quad (3.18)$$

From equating these two amplitudes, we obtain the conditions:

$$\tilde{\alpha}_{NN}^2 = 0, \quad (3.19)$$

$$\tilde{\alpha}_{HN} = -\frac{1}{32\pi^2\epsilon} (g_1^2 + 3g_2^2) \alpha_{HN}. \quad (3.20)$$

The one-loop divergence for $\bar{v}_L(p_1)N(p_2)H_0^*(p_3) \rightarrow H_0^*(p_4)H_0(p_5)$ at zero momentum reads

$$i\mathcal{M}_{\text{loop}} = \frac{i}{16\pi^2\epsilon} \bar{v}_1 \left[(12\lambda_H - g_1^2 - 3g_2^2 - 2Y_e^2) \alpha_{LNH} - 3g_1(g_1^2 + g_2^2) \alpha_{NB} \right. \\ \left. + 3g_2(g_1^2 + 3g_2^2 + 4Y_e^2) \alpha_{NW} + Y_e(3g_2^2 - 2\lambda_H - 2Y_e^2) \alpha_{HNe} \right] P_R u_2, \quad (3.21)$$

while in the EFT at tree level we have

$$i\mathcal{M}_{\text{div}} = -2i\tilde{\alpha}_{LNH}\bar{v}_1 P_R u_2. \quad (3.22)$$

This fixes

$$\tilde{\alpha}_{LNH} = \frac{1}{32\pi^2\epsilon} \left[3g_1(g_1^2 + g_2^2) \alpha_{NB} - 3g_2(g_1^2 + 3g_2^2 + 4Y_e^2) \alpha_{NW} \right. \\ \left. + Y_e(2\lambda_H - 3g_2^2 + 2Y_e^2) \alpha_{HNe} + (g_1^2 + 3g_2^2 - 12\lambda_H + 2Y_e^2) \alpha_{LNH} \right]. \quad (3.23)$$

Finally, upon computing the divergent part of $\bar{N}(p_1)e_R(p_2) \rightarrow H^-(p_3)H_0^*(p_4)$ at order $\mathcal{O}(p)$, we obtain:

$$i\mathcal{M}_{\text{loop}} = \frac{3i}{32\pi^2\epsilon} [g_1 Y_e \alpha_{NB} - 3g_2 Y_e \alpha_{NW} + (g_1^2 - g_2^2) \alpha_{HNe}] \bar{v}_1 (\not{p}_3 - \not{p}_4) P_R u_2, \quad (3.24)$$

and

$$i\mathcal{M}_{\text{div}} = i\tilde{\alpha}_{HNe}\bar{v}_1 (\not{p}_3 - \not{p}_4) P_R u_2, \quad (3.25)$$

which leads to

$$\tilde{\alpha}_{HNe} = \frac{3}{32\pi^2\epsilon} [g_1 Y_e \alpha_{NB} - 3g_2 Y_e \alpha_{NW} + (g_1^2 - g_2^2) \alpha_{HNe}]. \quad (3.26)$$

We provide a completely independent cross-check of these results in Appendix A.

To conclude, for the Z factors of the fields we have:

$$Z_H = 1 + \frac{1}{32\pi^2\epsilon} [g_1^2 + 3g_2^2 - 6 \text{Tr} (Y_u^2 + Y_d^2) - 2 \text{Tr} (Y_e^2)], \quad (3.27)$$

$$Z_L = 1 - \frac{1}{64\pi^2\epsilon} (g_1^2 + 3g_2^2 + 2Y_e^2), \quad (3.28)$$

$$Z_e = 1 - \frac{1}{16\pi^2\epsilon} (g_1^2 + Y_e^2), \quad (3.29)$$

$$Z_B = 1 - \frac{41g_1^2}{96\pi^2\epsilon}, \quad (3.30)$$

$$Z_W = 1 + \frac{19g_2^2}{96\pi^2\epsilon}. \quad (3.31)$$

Note that we use Y_e to refer both to a particular entry of the Yukawa matrix and to this matrix itself (when it comes inside the trace).

4 Anomalous dimensions

We remove the redundant operators (those in grey in Tab. 1) using the relations in Eqs. (2.17)–(2.24). This shifts the Wilson coefficients α_{NB} , α_{NW} and α_{HN} :

$$\tilde{\alpha}_{NB} \rightarrow \tilde{\alpha}_{NB} - \frac{g_1}{8} (\tilde{\alpha}_{LN}^2 - \tilde{\alpha}_{LN}^3) = \frac{1}{64\pi^2\epsilon} [(3g_2^2 - 2g_1^2 + 4Y_e^2) \alpha_{NB} + 9g_1g_2\alpha_{NW}], \quad (4.1)$$

$$\tilde{\alpha}_{NW} \rightarrow \tilde{\alpha}_{NW} + \frac{g_2}{8} (\tilde{\alpha}_{LN}^2 - \tilde{\alpha}_{LN}^3) = \frac{1}{64\pi^2\epsilon} [3g_1g_2\alpha_{NB} + (g_1^2 - 6g_2^2 - 4Y_e^2) \alpha_{NW}], \quad (4.2)$$

$$\begin{aligned} \tilde{\alpha}_{HN} &\rightarrow \tilde{\alpha}_{HN} - \frac{g_1}{2} (\tilde{\alpha}_{DN}^2 - \tilde{\alpha}_{DN}^3) - \frac{Y_e}{2} (\tilde{\alpha}_{LN}^2 - \tilde{\alpha}_{LN}^3) \\ &= -\frac{1}{96\pi^2\epsilon} [9g_1Y_e\alpha_{NB} - 27g_2Y_e\alpha_{NW} + (4g_1^2 + 9g_2^2) \alpha_{HN} + 6Y_e^2\alpha_{HN_e}]; \end{aligned} \quad (4.3)$$

α_{HN_e} and α_{LNH} (accidentally) remain unchanged.

This way, we fully determine the divergent Lagrangian

$$\mathcal{L}_{\text{div}} = \frac{1}{32\pi^2\Lambda^2\epsilon} \vec{\mathcal{O}}^T \cdot \mathcal{C} \cdot \vec{\alpha}, \quad (4.4)$$

where the vector $\vec{\mathcal{O}}$ encodes the relevant operators, and the matrix \mathcal{C} contains only SM couplings. We use the latter to fix the counterterms in the NSMEFT Lagrangian

$$\mathcal{L}_6 = \frac{1}{\Lambda^2} \vec{\alpha}^T \cdot \vec{\mathcal{O}} + \frac{1}{\Lambda^2} \vec{\mathcal{O}}^T \cdot (Z_F Z - \mathbb{1}) \cdot \vec{\alpha} \quad (4.5)$$

$$= \frac{1}{\Lambda^2} \vec{\alpha}^T \cdot \vec{\mathcal{O}} + \frac{1}{32\pi^2\Lambda^2\epsilon} \vec{\mathcal{O}}^T \cdot (K_F + K) \cdot \vec{\alpha}, \quad (4.6)$$

where Z_F contains the wave-function renormalisation factors ⁴, and we have introduced $Z = \mathbb{1} + K/(32\pi^2\epsilon)$ and $Z_F = \mathbb{1} + K_F/(32\pi^2\epsilon)$. We obtain

$$K = -(\mathcal{C} + K_F). \quad (4.7)$$

Following *e.g.* Ref. [47], it can be seen that the anomalous dimension matrix γ is simply given by K . Thus, we finally get

$$\gamma = \begin{pmatrix} \frac{91}{12}g_1^2 - \frac{9}{4}g_2^2 - \frac{3}{2}Y_e^2 + \text{Tr}^2 & -\frac{9}{2}g_1g_2 & 0 & 0 & 0 \\ -\frac{3}{2}g_1g_2 & -\frac{3}{4}g_1^2 - \frac{11}{12}g_2^2 + \frac{5}{2}Y_e^2 + \text{Tr}^2 & 0 & 0 & 0 \\ 3g_1Y_e & -9g_2Y_e & \frac{1}{3}g_1^2 + 2\text{Tr}^2 & 2Y_e^2 & 0 \\ -3g_1Y_e & 9g_2Y_e & 0 & -3g_1^2 + Y_e^2 + 2\text{Tr}^2 & 0 \\ -3g_1(g_1^2 + g_2^2) & 3g_2(g_1^2 + 3g_2^2 + 4Y_e^2) & 0 & Y_e(3g_2^2 - 2\lambda_H - 2Y_e^2) & -\frac{9}{4}g_1^2 - \frac{27}{4}g_2^2 + 12\lambda_H - \frac{3}{2}Y_e^2 + 3\text{Tr}^2 \end{pmatrix} \begin{matrix} \alpha_{NB} \\ \alpha_{NW} \\ \alpha_{HN} \\ \alpha_{HNe} \\ \alpha_{LNH} \end{matrix}, \quad (4.8)$$

where we have defined

$$\text{Tr}^2 \equiv 3\text{Tr}(Y_u^2 + Y_d^2) + \text{Tr}(Y_e^2). \quad (4.9)$$

We notice that, as anticipated in section 2, the operators \mathcal{O}_{HN} , \mathcal{O}_{HNe} and \mathcal{O}_{LNH} do not mix in the limit of vanishing Y_e . Also, these operators, which can be generated at tree level in UV completions of the SM, do not renormalise \mathcal{O}_{NW} and \mathcal{O}_{NB} , which can only arise at one loop. We also stress that some entries, *e.g.* the renormalisation of \mathcal{O}_{HN} by \mathcal{O}_{NW} , are enhanced with respect to the naive dimensional analysis estimation by up to an order of magnitude.

5 Some phenomenological implications

Among the variety of phenomenological implications, we would like to explore the possibility that the excess of low-energy electron recoil events recently observed by XENON1T [6], which has triggered a lot of attention [48–71], is due to a relatively large neutrino magnetic dipole moment. Following Ref. [72] (see also Ref. [52]), one can take $\mu_\nu \sim 2 \times 10^{-11} \mu_B$, where μ_B stands for the Bohr magneton. (This explanation necessarily assumes that the strong astrophysical bounds [73], which are subject to a number of uncontrollable uncertainties, can not be taken at face value.)

The neutrino magnetic moment can also be expressed as [43]

$$\left| \frac{\mu_\nu}{\mu_B} \right| = \frac{4\sqrt{2} m_e v}{e \Lambda^2} \alpha_{NA}(v), \quad (5.1)$$

⁴Explicitly,

$$Z_F = \text{diag} \left(\sqrt{Z_L Z_H Z_B}, \sqrt{Z_L Z_H Z_W}, Z_H, \sqrt{Z_E Z_H}, \sqrt{Z_L} (Z_H)^{3/2} \right).$$

where $\alpha_{NA} = c_W \alpha_{NB} + s_W \alpha_{NW}$, m_e represents the electron mass and $e = \sqrt{4\pi\alpha_{\text{QED}}}$ with α_{QED} the electromagnetic fine-structure constant. The non detection of new particles at the LHC most likely implies that α_{NA} is generated at a scale $\Lambda \gtrsim \text{TeV}$. In what follows we assume two benchmark values of $\Lambda = 1 \text{ TeV}$ and 100 TeV . We obtain

$$\alpha_{NA} \sim 9 \times 10^{-6} \quad (9 \times 10^{-2}) \quad \text{for } \Lambda = 1 \text{ TeV} \quad (100 \text{ TeV}). \quad (5.2)$$

Even if this is the only non-vanishing Wilson coefficient at the high scale, running down from $\Lambda = 1 \text{ TeV}$ (100 TeV) to the EW scale, we obtain:

$$|\alpha_{LNH}(v)| \sim 6 \times 10^{-8} \quad (2 \times 10^{-3}), \quad (5.3)$$

$$|\alpha_{HN}(v)| \sim 10^{-9} \quad (6 \times 10^{-5}), \quad (5.4)$$

$$|\alpha_{NZ}(v)| \sim 2 \times 10^{-8} \quad (7 \times 10^{-4}), \quad (5.5)$$

where $\alpha_{NZ} = c_W \alpha_{NW} - s_W \alpha_{NB}$. (We have assumed that all neutrinos have similar magnetic moment, so α_{HN} is only suppressed by the tau Yukawa.)

An immediate consequence of this result is that the neutrino masses get a radiative contribution of order $\delta m_\nu = |\alpha_{LNH}|v^3/(2\sqrt{2}\Lambda^2) \sim 3 \times 10^2 \text{ eV}$ (10^3 eV) for the new physics scale $\Lambda = 1 \text{ TeV}$ (100 TeV). Most of this correction must be cancelled by the bare Y_N , implying a fine-tuning of order $\mathcal{O}(10^3 - 10^4)$. This observation was already made in Ref. [43]. The authors of this article obtain the RGEs of α_{NB} , α_{NW} and α_{LNH} neglecting the Yukawa terms. The equivalent block in our γ matches their result up to a factor of 2 in the mixing of α_{NB} and α_{NW} into α_{LNH} , which (slightly) weakens the amount of fine-tuning. Unfortunately, we do not find enough details about the computation in Ref. [43] to disentangle the root of this discrepancy.

Irrespectively of this tuning, given the aforementioned numbers for the Wilson coefficients and taking into account the three lepton families, we predict the following Higgs and Z decays for $\Lambda = 1 \text{ TeV}$ (100 TeV):

$$\Gamma(h \rightarrow \text{inv}) = \frac{3m_h v^4}{16\pi\Lambda^4} \alpha_{LNH}^2 \sim 9 \times 10^{-14} \text{ MeV} \quad (2 \times 10^{-12} \text{ MeV}), \quad (5.6)$$

$$\Gamma(Z \rightarrow \text{inv}) = \frac{m_Z^3 v^2}{8\pi\Lambda^4} (\alpha_{HN}^2 + 2\alpha_{NZ}^2) \sim 10^{-18} \text{ GeV} \quad (2 \times 10^{-17} \text{ GeV}). \quad (5.7)$$

The expected Higgs and Z branching ratios are therefore

$$\mathcal{B}(h \rightarrow \text{inv}) \sim 2 \times 10^{-14} \quad (4 \times 10^{-13}), \quad (5.8)$$

$$\mathcal{B}(Z \rightarrow \text{inv}) \sim 5 \times 10^{-19} \quad (8 \times 10^{-18}), \quad (5.9)$$

where we have used $\Gamma_h^{\text{total}} \approx 4 \text{ MeV}$ and $\Gamma_Z^{\text{total}} \approx 2.49 \text{ GeV}$ [74]. Unfortunately, these numbers are so small that it is not feasible that they will be tested at any current or future facilities [75].

On a different front, from Eq. (4.8) it is also clear that \mathcal{O}_{HNe} generates a contribution δm_ν to the neutrino mass too. For the tau flavour, requiring $\delta m_\nu < 1$ eV, it can be shown that $\alpha_{HNe} \lesssim 2 \times 10^{-6}$ for $\Lambda = 1$ TeV. If α_{HNe} is rather generated at $\Lambda = 100$ TeV, we obtain $\alpha_{HNe} \lesssim 2 \times 10^{-2}$. These bounds surpass by orders of magnitude the best bound that can be set on α_{HNe} using measurements of W branching ratios, which is $\mathcal{O}(1)$ ⁵.

6 Conclusions

We have computed the RGEs of all dimension-six Higgs operators in the NSMEFT at one loop, thereby extending previous partial computations which did not include all the operators nor the Yukawa dependence. Thus, this work comprises a substantial step forward towards the description of new physics in terms of EFTs in the regime in which neutrinos are Dirac particles.

In our basis, the only operators that do not mix among themselves under running are \mathcal{O}_{HN} and \mathcal{O}_{LNH} , while the three operators \mathcal{O}_{HN} , \mathcal{O}_{HNe} and \mathcal{O}_{LNH} renormalise independently in the limit of vanishing Yukawas (even at higher orders).

The operators \mathcal{O}_{NB} and \mathcal{O}_{NW} , which together contribute to the neutrino magnetic dipole moment, renormalise \mathcal{O}_{LNH} via gauge interactions; all the others are Yukawa suppressed. With this in mind, we have also analysed the consequences of the recent XENON1T excess [6] being due to an anomalous Dirac neutrino magnetic dipole moment $\mu_\nu \sim 2 \times 10^{-11} \mu_B$. We observe that:

1. A contribution to the neutrino mass of order 10^2 – 10^3 eV would be generated, requiring a sensible cancellation between this and the bare mass to account for the tiny observed $m_\nu \sim 0.1$ eV. This was already pointed out in Ref. [43]. We however find a small discrepancy with the result in this reference; see section 5.
2. Irrespectively of whether neutrino masses are tuned, \mathcal{O}_{LNH} would be induced radiatively triggering the Higgs decay to invisible $h \rightarrow \text{inv}$ with branching ratio of order $\sim 2 \times 10^{-14}$ (4×10^{-13}) for $\Lambda = 1$ TeV (100 TeV).
3. If the dipole moment of the electron and tau neutrinos are equally large, then one also expects a new contribution to the invisible Z decay with branching ratio 5×10^{-19} (8×10^{-18}) for $\Lambda = 1$ TeV (100 TeV).

⁵Note that assuming $\alpha_{NW} = 0$,

$$\Delta\Gamma(W \rightarrow \ell\nu) = \frac{m_W^3 v^2}{48\pi\Lambda^4} \alpha_{HNe}^2,$$

while experimentally this quantity is bounded to $\Delta\Gamma(W \rightarrow \ell\nu)/\Gamma_W^{\text{total}} < 2 \times 10^{-3}$ at the 95% CL [74], with $\Gamma_W^{\text{total}} \sim 2.09$ GeV. Altogether this implies $|\alpha_{HNe}/\Lambda^2| \lesssim 4.5$ TeV⁻².

Unfortunately, even if the XENON1T excess survives in the long term, these numbers are too small to be explored at current and near future facilities.

On a different note, we have shown that \mathcal{O}_{HN_e} also renormalises the neutrino mass term by δm_ν . Despite being Yukawa suppressed, we find that requiring $\delta m_\nu < 1$ eV sets a bound on α_{HN_e} orders of magnitude stronger than the current bound based on limits from $W \rightarrow \ell\nu$.

Acknowledgements

We would like to thank Claudius Krause and Jose Santiago for useful discussions. MC is supported by the Spanish MINECO under the Juan de la Cierva programme as well as by the Ministry of Science and Innovation under grant number FPA2016-78220-C3-3-P, and by the Junta de Andalucía grants FQM 101 and A-FQM-211-UGR18 (fondos FEDER).

A Cross-checks

Our partial yet thorough cross-check consists in computing the gauge dependence of UV divergences in the sector of α_{HN} , α_{HN_e} and α_{LNH} , evaluating by hand (with the help of `FeynRules` [76]) each of the diagrams generated with `QGRAF` [77].

We will make use of the following identities [42]:

$$\int \frac{d^d k}{(2\pi)^d} \frac{1}{(k^2 - M^2)^n} = A_n, \quad (\text{A.1})$$

$$\int \frac{d^d k}{(2\pi)^d} \frac{k^\mu k^\nu}{(k^2 - M^2)^n} = g^{\mu\nu} B_n, \quad (\text{A.2})$$

$$\int \frac{d^d k}{(2\pi)^d} \frac{k^\mu k^\nu k^\rho k^\sigma}{(k^2 - M^2)^n} = (g^{\mu\nu} g^{\rho\sigma} + g^{\mu\rho} g^{\nu\sigma} + g^{\mu\sigma} g^{\nu\rho}) C_n, \quad (\text{A.3})$$

that lead to

$$A_2 = \frac{i}{16\pi^2\epsilon} + \dots, \quad (\text{A.4})$$

$$B_3 = \frac{i}{64\pi^2\epsilon} + \dots, \quad (\text{A.5})$$

$$C_4 = \frac{i}{384\pi^2\epsilon} + \dots, \quad (\text{A.6})$$

where the ellipses encode finite terms.

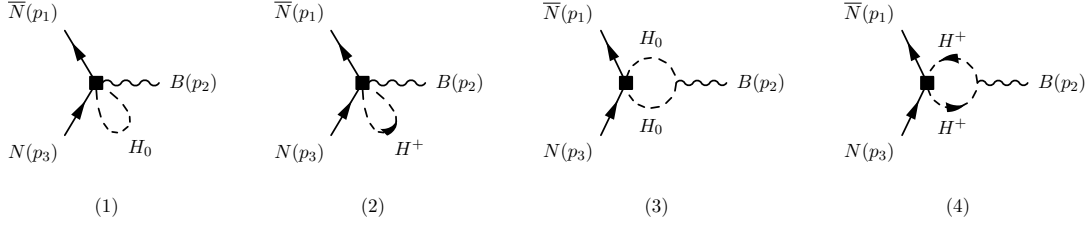


Figure 1: *Relevant Feynman diagrams for $\bar{N}N \rightarrow B$.*

A.1 $\bar{N}N \rightarrow B$

The relevant diagrams are given in Fig. 1. The different contributions to the amplitude read:

$$i\mathcal{M}_1 = g_1 \alpha_{HN} A_1 \bar{v}_1 \gamma^\mu P_R u_3 \epsilon_\mu^*, \quad (\text{A.7})$$

$$\mathcal{M}_2 = \mathcal{M}_1, \quad (\text{A.8})$$

$$i\mathcal{M}_3 = -\frac{g_1}{2} \alpha_{HN} \bar{v}_1 \left[4B_2 \gamma^\mu + (16C_4 - 4B_3) p_2^2 \gamma^\mu + (A_2 - 8B_3 + 32C_4) p_2^\mu \not{p}_2 \right] P_R u_3 \epsilon_\mu^*, \quad (\text{A.9})$$

$$\mathcal{M}_4 = \mathcal{M}_3. \quad (\text{A.10})$$

Here and in what follows $v_1 \equiv v(p_1)$, $u_3 \equiv u(p_3)$ and $\epsilon_\mu^* \equiv \epsilon_\mu^*(-p_2)$.

Summing over the four diagrams we obtain

$$i\mathcal{M}_{\text{loop}} = \frac{i}{48\pi^2 \epsilon} g_1 \alpha_{HN} \bar{v}_1 \left(p_2^2 \gamma^\mu - p_2^\mu \not{p}_2 \right) P_R u_3 \epsilon_\mu^*. \quad (\text{A.11})$$

The `FeynArts/FormCalc` convention for momenta differs from our setup involving `QGRAF` and `FeynRules`. In the former, the momenta of incoming particles point in and outgoing particles point out, while in the second all momenta point in. The momentum associated to each particle also differs.

Thus, we have $p_3^{\text{FC}} = -p_2^{\text{QG}}$, $p_1^{\text{FC}} = p_1^{\text{QG}}$ and $p_2^{\text{FC}} = p_3^{\text{QG}}$. Having this in mind, it is evident that this result agrees with Eq. (3.1) in the limit $Y_e, \alpha_{NB}, \alpha_{NW} \rightarrow 0$.

A.2 $\bar{\nu}_L N \rightarrow H_0$

The relevant diagrams are shown in Fig. 2⁶. We have:

$$\mathcal{M}_2 = 0, \quad (\text{A.12})$$

⁶In what follows the “missing” diagrams are either of order $\mathcal{O}(\alpha_{NB, NW})$ or $\mathcal{O}(1/\Lambda^4)$. This is why we do not display them.

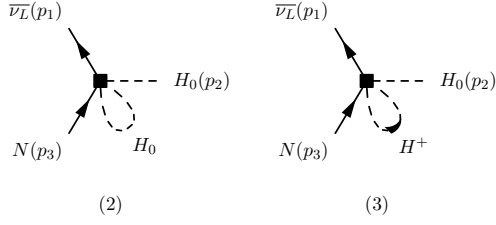


Figure 2: *Relevant Feynman diagrams for $\bar{\nu}_L N \rightarrow H_0$.*

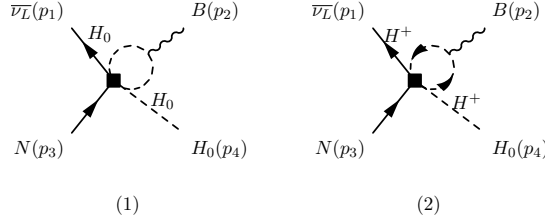


Figure 3: *Relevant Feynman diagrams for $\bar{\nu}_L N \rightarrow B H_0$.*

$$\mathcal{M}_3 = 0. \tag{A.13}$$

Obviously, within our approximation this result agrees with Eq. (3.5), which only depends on α_{NB} and α_{NW} (and on α_{HN_e} through Y_e).

A.3 $\bar{\nu}_L N \rightarrow B H_0$

The two relevant diagrams are those in Fig. 3. We obtain trivially

$$\mathcal{M}_1 = 0, \tag{A.14}$$

$$\mathcal{M}_2 = 0. \tag{A.15}$$

This again matches Eq. (3.11) given our approximations.

A.4 $\bar{e}_L N \rightarrow W^3 H^+$

In this case we have the two diagrams of Fig. 4, which lead to

$$\mathcal{M}_3 = 0, \tag{A.16}$$

$$\mathcal{M}_4 = 0, \tag{A.17}$$

in agreement (within our approximation) with Eq. (3.14).

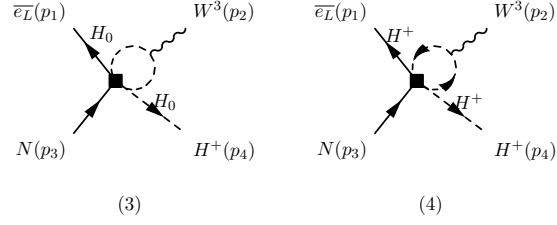


Figure 4: *Relevant Feynman diagrams for $\bar{e}_L N \rightarrow W^3 H^+$.*

A.5 $\bar{N} N \rightarrow H_0^* H_0$

We have eleven relevant Feynman diagrams for this amplitude. They are depicted in Fig. 5. The different contributions read:

$$i\mathcal{M}_1 = g_1^2 (A_2 - B_3) \alpha_{HN} \bar{v}_1 \not{p}_2 P_R u_3, \quad (\text{A.18})$$

$$i\mathcal{M}_2 = g_2^2 (A_2 - B_3) \alpha_{HN} \bar{v}_1 \not{p}_2 P_R u_3, \quad (\text{A.19})$$

$$i\mathcal{M}_3 = g_2^2 (A_2 + 2B_3) \alpha_{HN} \bar{v}_1 \not{p}_2 P_R u_3, \quad (\text{A.20})$$

$$i\mathcal{M}_4 = -\frac{g_1^2}{2} (A_2 + 2B_3) \alpha_{HN} \bar{v}_1 \not{p}_4 P_R u_3, \quad (\text{A.21})$$

$$i\mathcal{M}_5 = -\frac{g_2^2}{2} (A_2 + 2B_3) \alpha_{HN} \bar{v}_1 \not{p}_4 P_R u_3, \quad (\text{A.22})$$

$$i\mathcal{M}_6 = -g_2^2 (A_2 + 2B_3) \alpha_{HN} \bar{v}_1 \not{p}_4 P_R u_3, \quad (\text{A.23})$$

$$i\mathcal{M}_7 = 2\lambda_H (A_2 - 4B_3) \alpha_{HN} \bar{v}_1 (\not{p}_2 + \not{p}_4) P_R u_3, \quad (\text{A.24})$$

$$i\mathcal{M}_8 = \lambda_H (A_2 - 4B_3) \alpha_{HN} \bar{v}_1 (\not{p}_2 + \not{p}_4) P_R u_3, \quad (\text{A.25})$$

$$i\mathcal{M}_{15} = -\frac{g_1^2}{4} A_2 \alpha_{HN} \bar{v}_1 (\not{p}_2 - \not{p}_4) P_R u_3, \quad (\text{A.26})$$

$$i\mathcal{M}_{16} = -\frac{g_2^2}{4} A_2 \alpha_{HN} \bar{v}_1 (\not{p}_2 - \not{p}_4) P_R u_3, \quad (\text{A.27})$$

$$i\mathcal{M}_{17} = -\frac{g_2^2}{2} A_2 \alpha_{HN} \bar{v}_1 (\not{p}_2 - \not{p}_4) P_R u_3. \quad (\text{A.28})$$

Summing over all them we arrive at

$$i\mathcal{M}_{\text{loop}} = \frac{i}{32\pi^2\epsilon} (g_1^2 + 3g_2^2) \alpha_{HN} \bar{v}_1 (\not{p}_2 - \not{p}_4) P_R u_3. \quad (\text{A.29})$$

In this case, $p_1^{\text{FC}} = p_1^{\text{QG}}$, $p_2^{\text{FC}} = p_3^{\text{QG}}$, $p_3^{\text{FC}} = -p_2^{\text{QG}}$ and $p_4^{\text{FC}} = -p_4^{\text{QG}}$. Using this information, we match precisely Eq. (3.17).

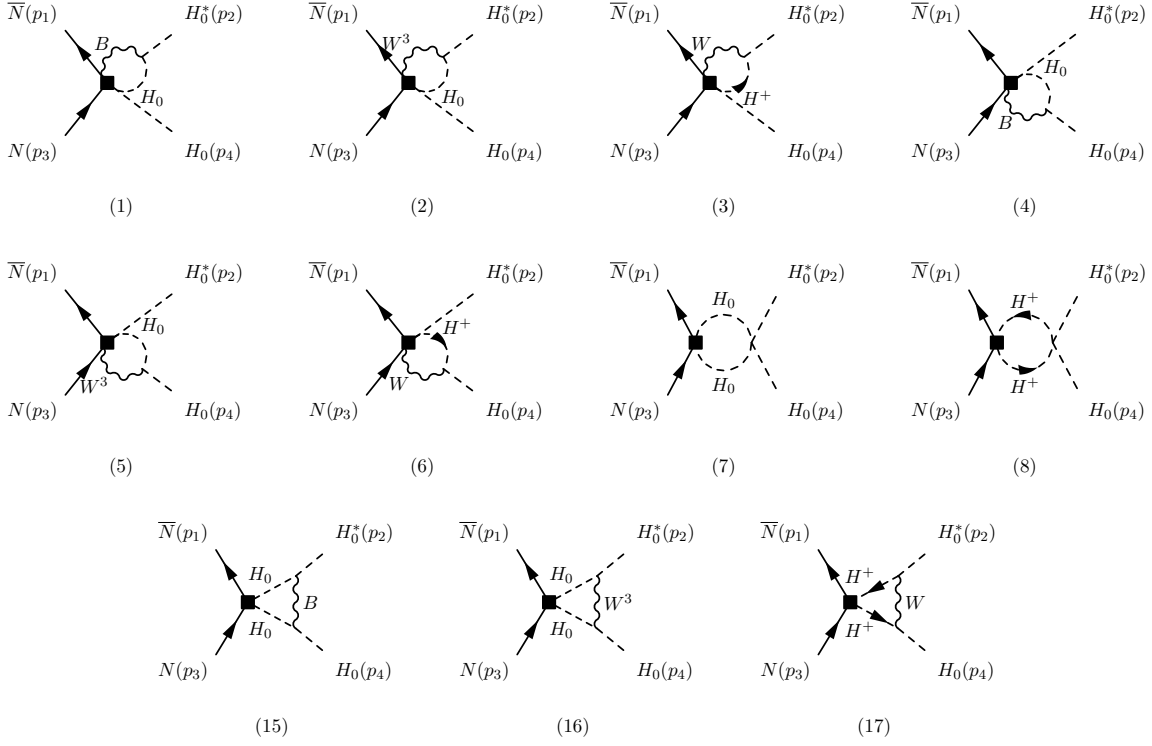


Figure 5: *Relevant Feynman diagrams for $\bar{N}N \rightarrow H_0^*H_0$.*

A.6 $\bar{\nu}_L N H_0^* \rightarrow H_0^* H_0$

21 diagrams need to be computed in this case. They are all shown in Fig. 6. We have:

$$i\mathcal{M}_9 = 4\lambda_H A_2 \alpha_{LNH} \bar{\nu}_1 P_R u_3, \quad (\text{A.30})$$

$$\mathcal{M}_{10} = \frac{1}{4} \mathcal{M}_9, \quad (\text{A.31})$$

$$\mathcal{M}_{11} = \frac{1}{2} \mathcal{M}_9, \quad (\text{A.32})$$

$$\mathcal{M}_{13} = \mathcal{M}_9, \quad (\text{A.33})$$

$$\mathcal{M}_{14} = \frac{1}{4} \mathcal{M}_9, \quad (\text{A.34})$$

$$i\mathcal{M}_{15} = -\frac{g_1^2}{2} A_2 \alpha_{LNH} \bar{\nu}_1 P_R u_3, \quad (\text{A.35})$$

$$i\mathcal{M}_{16} = -\frac{g_2^2}{2} A_2 \alpha_{LNH} \bar{\nu}_1 P_R u_3, \quad (\text{A.36})$$

$$\mathcal{M}_{17} = \mathcal{M}_{16}, \quad (\text{A.37})$$

$$\mathcal{M}_{18} = -\mathcal{M}_{15}, \quad (\text{A.38})$$

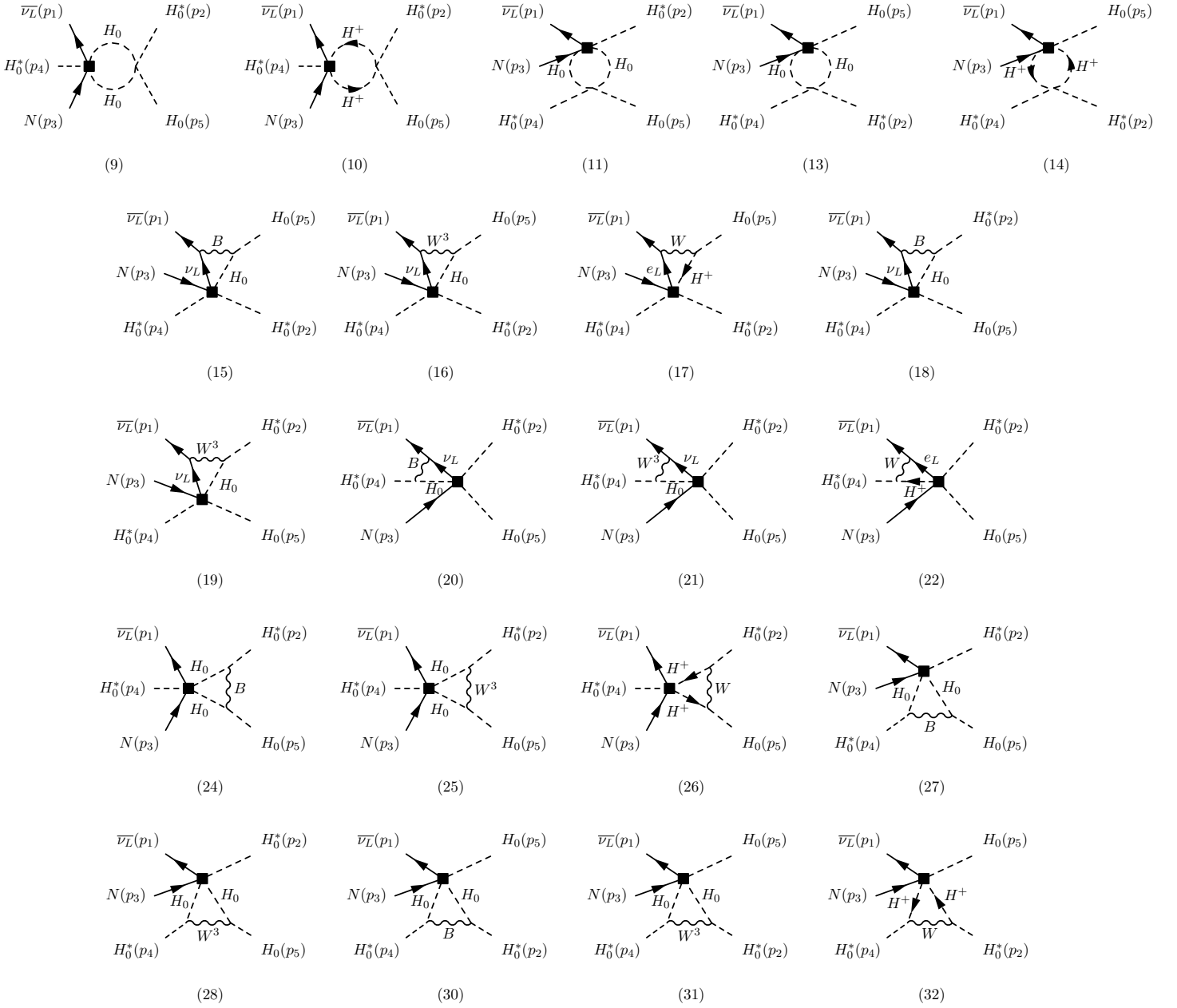


Figure 6: *Relevant Feynman diagrams for $\bar{\nu}_L N H_0^* \rightarrow H_0^* H_0$.*

$$\mathcal{M}_{19} = -\mathcal{M}_{16}, \quad (\text{A.39})$$

$$\mathcal{M}_{20} = \mathcal{M}_{15}, \quad (\text{A.40})$$

$$\mathcal{M}_{21} = \mathcal{M}_{16}, \quad (\text{A.41})$$

$$\mathcal{M}_{22} = \mathcal{M}_{16}, \quad (\text{A.42})$$

$$\mathcal{M}_{24} = \mathcal{M}_{15}, \quad (\text{A.43})$$

$$\mathcal{M}_{25} = \mathcal{M}_{16}, \quad (\text{A.44})$$

$$\mathcal{M}_{26} = \mathcal{M}_{16}, \quad (\text{A.45})$$

$$\mathcal{M}_{27} = -\mathcal{M}_{15}, \quad (\text{A.46})$$

$$\mathcal{M}_{28} = -\mathcal{M}_{16}, \quad (\text{A.47})$$

$$\mathcal{M}_{30} = \mathcal{M}_{15}, \quad (\text{A.48})$$

$$\mathcal{M}_{31} = \mathcal{M}_{16}, \quad (\text{A.49})$$

$$\mathcal{M}_{32} = \mathcal{M}_{16}. \quad (\text{A.50})$$

As a result, we obtain

$$i\mathcal{M}_{\text{loop}} = \frac{i}{16\pi^2\epsilon} (12\lambda_H - g_1^2 - 3g_2^2) \alpha_{LNH} \bar{v}_1 P_R u_3, \quad (\text{A.51})$$

in agreement (within our approximation) with Eq. (3.21).

A.7 $\bar{N}e_R \rightarrow H^- H_0^*$

Finally, this amplitude splits into the ten diagrams of Fig. 7. We have

$$i\mathcal{M}_1 = 2g_2^2 (A_2 - B_3) \alpha_{HN_e} \bar{v}_1 \not{p}_2 P_R u_3, \quad (\text{A.52})$$

$$\mathcal{M}_2 = \frac{1}{2} \mathcal{M}_1, \quad (\text{A.53})$$

$$i\mathcal{M}_3 = -2g_2^2 (A_2 - B_3) \alpha_{HN_e} \bar{v}_1 \not{p}_4 P_R u_3, \quad (\text{A.54})$$

$$\mathcal{M}_4 = \frac{1}{2} \mathcal{M}_3, \quad (\text{A.55})$$

$$i\mathcal{M}_5 = -\lambda_H (A_2 - 4B_3) \alpha_{HN_e} \bar{v}_1 (\not{p}_2 + \not{p}_4) P_R u_3, \quad (\text{A.56})$$

$$i\mathcal{M}_8 = -g_1^2 \alpha_{HN_e} \bar{v}_1 \left[(A_2 + B_3) \not{p}_2 + \frac{1}{2} A_2 (\not{p}_3 - \not{p}_4) \right] P_R u_3, \quad (\text{A.57})$$

$$i\mathcal{M}_9 = g_1^2 \alpha_{HN_e} \bar{v}_1 \left[(A_2 + B_3) \not{p}_4 + \frac{1}{2} A_2 (\not{p}_3 - \not{p}_2) \right] P_R u_3, \quad (\text{A.58})$$

$$i\mathcal{M}_{10} = -\frac{1}{2} g_2^2 A_2 \alpha_{HN_e} \bar{v}_1 (\not{p}_2 - \not{p}_4) P_R u_3, \quad (\text{A.59})$$

$$i\mathcal{M}_{11} = \frac{1}{4} g_1^2 A_2 \alpha_{HN_e} \bar{v}_1 (\not{p}_2 - \not{p}_4) P_R u_3, \quad (\text{A.60})$$

$$\mathcal{M}_{12} = \frac{1}{2} \mathcal{M}_{10}. \quad (\text{A.61})$$

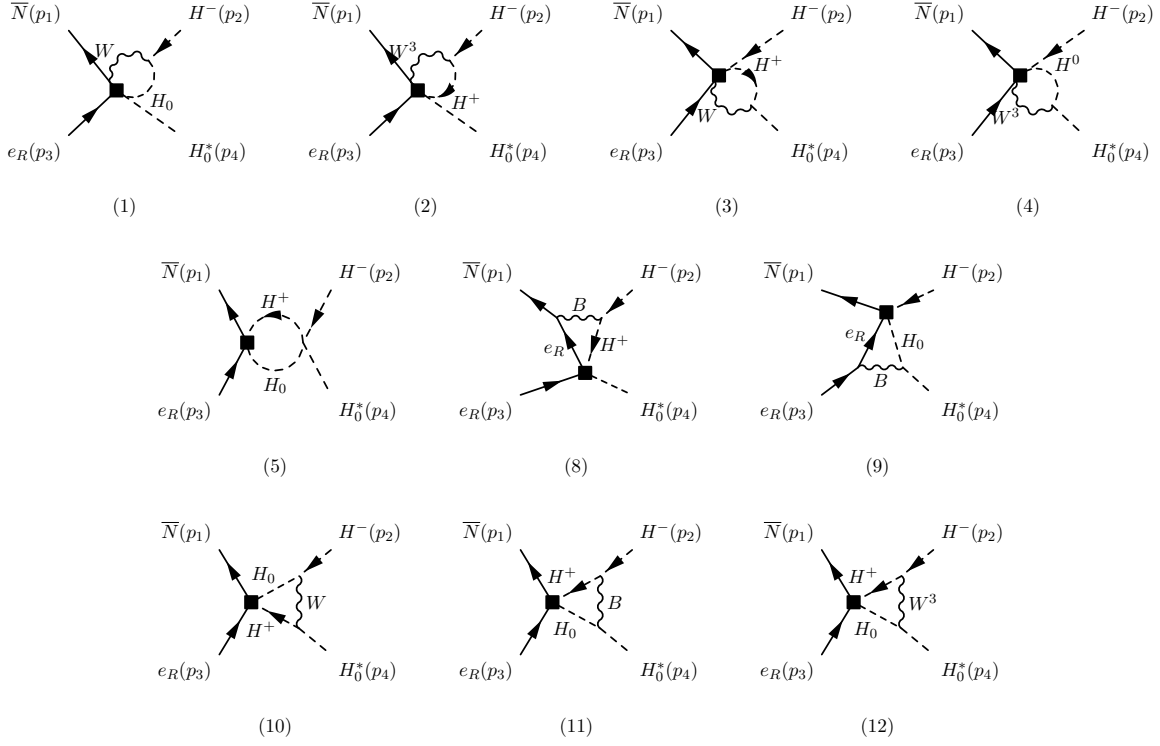


Figure 7: *Relevant Feynman diagrams for $\bar{N}e_R \rightarrow H^- H_0^*$.*

Thus, we finally obtain:

$$i\mathcal{M}_{\text{loop}} = -\frac{3i}{32\pi^2\epsilon} (g_1^2 - g_2^2) \alpha_{HN e \bar{\nu}_1} (\not{p}_2 - \not{p}_4) P_R u_3. \quad (\text{A.62})$$

In this case, $p_1^{\text{FC}} = p_1^{\text{QG}}$, $p_2^{\text{FC}} = p_3^{\text{QG}}$, $p_3^{\text{FC}} = -p_2^{\text{QG}}$, and $p_4^{\text{FC}} = -p_4^{\text{QG}}$. So we easily see that we match Eq. (3.24).

References

- [1] W. Buchmuller and D. Wyler, *Effective Lagrangian Analysis of New Interactions and Flavor Conservation*, *Nucl. Phys.* **B268** (1986) 621.
- [2] B. Grzadkowski, M. Iskrzynski, M. Misiak and J. Rosiek, *Dimension-Six Terms in the Standard Model Lagrangian*, *JHEP* **10** (2010) 085 [1008.4884].
- [3] I. Brivio and M. Trott, *The Standard Model as an Effective Field Theory*, *Phys. Rept.* **793** (2019) 1 [1706.08945].

- [4] CMS collaboration, *Angular analysis of the decay $B^0 \rightarrow K^{*0} \mu^+ \mu^-$ from pp collisions at $\sqrt{s} = 8$ TeV*, *Phys. Lett. B* **753** (2016) 424 [1507.08126].
- [5] CMS collaboration, *Measurement of angular parameters from the decay $B^0 \rightarrow K^{*0} \mu^+ \mu^-$ in proton-proton collisions at $\sqrt{s} = 8$ TeV*, *Phys. Lett. B* **781** (2018) 517 [1710.02846].
- [6] XENON collaboration, *Observation of Excess Electronic Recoil Events in XENON1T*, 2006.09721.
- [7] C. Grojean, E. E. Jenkins, A. V. Manohar and M. Trott, *Renormalization Group Scaling of Higgs Operators and $\Gamma(h \rightarrow \gamma\gamma)$* , *JHEP* **04** (2013) 016 [1301.2588].
- [8] J. Elias-Miro, J. Espinosa, E. Masso and A. Pomarol, *Renormalization of dimension-six operators relevant for the Higgs decays $h \rightarrow \gamma\gamma, \gamma Z$* , *JHEP* **08** (2013) 033 [1302.5661].
- [9] J. Elias-Miro, J. Espinosa, E. Masso and A. Pomarol, *Higgs windows to new physics through $d=6$ operators: constraints and one-loop anomalous dimensions*, *JHEP* **11** (2013) 066 [1308.1879].
- [10] E. E. Jenkins, A. V. Manohar and M. Trott, *Renormalization Group Evolution of the Standard Model Dimension Six Operators I: Formalism and λ Dependence*, *JHEP* **10** (2013) 087 [1308.2627].
- [11] E. E. Jenkins, A. V. Manohar and M. Trott, *Renormalization Group Evolution of the Standard Model Dimension Six Operators II: Yukawa Dependence*, *JHEP* **01** (2014) 035 [1310.4838].
- [12] R. Alonso, E. E. Jenkins, A. V. Manohar and M. Trott, *Renormalization Group Evolution of the Standard Model Dimension Six Operators III: Gauge Coupling Dependence and Phenomenology*, *JHEP* **04** (2014) 159 [1312.2014].
- [13] Y. Liao and X.-D. Ma, *Renormalization Group Evolution of Dimension-seven Operators in Standard Model Effective Field Theory and Relevant Phenomenology*, *JHEP* **03** (2019) 179 [1901.10302].
- [14] E. E. Jenkins, A. V. Manohar and P. Stoffer, *Low-Energy Effective Field Theory below the Electroweak Scale: Anomalous Dimensions*, *JHEP* **01** (2018) 084 [1711.05270].
- [15] E. E. Jenkins, A. V. Manohar and P. Stoffer, *Low-Energy Effective Field Theory below the Electroweak Scale: Operators and Matching*, *JHEP* **03** (2018) 016 [1709.04486].

- [16] W. Dekens and P. Stoffer, *Low-energy effective field theory below the electroweak scale: matching at one loop*, *JHEP* **10** (2019) 197 [1908.05295].
- [17] B. Henning, X. Lu and H. Murayama, *How to use the Standard Model effective field theory*, *JHEP* **01** (2016) 023 [1412.1837].
- [18] B. Henning, X. Lu and H. Murayama, *One-loop Matching and Running with Covariant Derivative Expansion*, *JHEP* **01** (2018) 123 [1604.01019].
- [19] S. A. R. Ellis, J. Quevillon, T. You and Z. Zhang, *Mixed heavy–light matching in the Universal One-Loop Effective Action*, *Phys. Lett.* **B762** (2016) 166 [1604.02445].
- [20] J. Fuentes-Martin, J. Portoles and P. Ruiz-Femenia, *Integrating out heavy particles with functional methods: a simplified framework*, *JHEP* **09** (2016) 156 [1607.02142].
- [21] Z. Zhang, *Covariant diagrams for one-loop matching*, *JHEP* **05** (2017) 152 [1610.00710].
- [22] S. A. R. Ellis, J. Quevillon, T. You and Z. Zhang, *Extending the Universal One-Loop Effective Action: Heavy-Light Coefficients*, *JHEP* **08** (2017) 054 [1706.07765].
- [23] F. del Aguila, Z. Kunszt and J. Santiago, *One-loop effective lagrangians after matching*, *Eur. Phys. J.* **C76** (2016) 244 [1602.00126].
- [24] J. C. Criado, *MatchingTools: a Python library for symbolic effective field theory calculations*, *Comput. Phys. Commun.* **227** (2018) 42 [1710.06445].
- [25] S. Das Bakshi, J. Chakraborty and S. K. Patra, *CoDEx: Wilson coefficient calculator connecting SMEFT to UV theory*, *Eur. Phys. J.* **C79** (2019) 21 [1808.04403].
- [26] I. Brivio et al., *Computing Tools for the SMEFT*, in *Computing Tools for the SMEFT*, J. Aebischer, M. Fael, A. Lenz, M. Spannowsky and J. Virto, eds., 2019, 1910.11003.
- [27] V. Gherardi, D. Marzocca and E. Venturini, *Matching scalar leptiquarks to the SMEFT at one loop*, 2003.12525.
- [28] L. E. Ibanez, V. Martin-Lozano and I. Valenzuela, *Constraining Neutrino Masses, the Cosmological Constant and BSM Physics from the Weak Gravity Conjecture*, *JHEP* **11** (2017) 066 [1706.05392].
- [29] N. Arkani-Hamed, S. Dubovsky, A. Nicolis and G. Villadoro, *Quantum Horizons of the Standard Model Landscape*, *JHEP* **06** (2007) 078 [hep-th/0703067].

- [30] H. Ooguri and C. Vafa, *Non-supersymmetric AdS and the Swampland*, *Adv. Theor. Math. Phys.* **21** (2017) 1787 [1610.01533].
- [31] F. del Aguila, S. Bar-Shalom, A. Soni and J. Wudka, *Heavy Majorana Neutrinos in the Effective Lagrangian Description: Application to Hadron Colliders*, *Phys. Lett.* **B670** (2009) 399 [0806.0876].
- [32] Y. Liao and X.-D. Ma, *Operators up to Dimension Seven in Standard Model Effective Field Theory Extended with Sterile Neutrinos*, *Phys. Rev.* **D96** (2017) 015012 [1612.04527].
- [33] L. Duarte, J. Peressutti and O. A. Sampayo, *Majorana neutrino decay in an Effective Approach*, *Phys. Rev.* **D92** (2015) 093002 [1508.01588].
- [34] L. Duarte, J. Peressutti and O. A. Sampayo, *Not-that-heavy Majorana neutrino signals at the LHC*, *J. Phys.* **G45** (2018) 025001 [1610.03894].
- [35] J. Alcaide, S. Banerjee, M. Chala and A. Titov, *Probes of the Standard Model effective field theory extended with a right-handed neutrino*, *JHEP* **08** (2019) 031 [1905.11375].
- [36] J. M. Butterworth, M. Chala, C. Englert, M. Spannowsky and A. Titov, *Higgs phenomenology as a probe of sterile neutrinos*, *Phys. Rev.* **D100** (2019) 115019 [1909.04665].
- [37] Y. Cai, T. Han, T. Li and R. Ruiz, *Lepton Number Violation: Seesaw Models and Their Collider Tests*, *Front. in Phys.* **6** (2018) 40 [1711.02180].
- [38] I. Bischer and W. Rodejohann, *General neutrino interactions from an effective field theory perspective*, *Nucl. Phys. B* **947** (2019) 114746 [1905.08699].
- [39] W. Dekens, J. de Vries, K. Fuyuto, E. Mereghetti and G. Zhou, *Sterile neutrinos and neutrinoless double beta decay in effective field theory*, 2002.07182.
- [40] P. D. Bolton, F. F. Deppisch and C. Hati, *Probing New Physics with Long-Range Neutrino Interactions: An Effective Field Theory Approach*, 2004.08328.
- [41] L. Duarte, G. Zapata and O. Sampayo, *Angular and polarization observables for Majorana-mediated B decays with effective interactions*, 2006.11216.
- [42] M. Chala and A. Titov, *One-loop matching in the SMEFT extended with a sterile neutrino*, *JHEP* **05** (2020) 139 [2001.07732].
- [43] N. F. Bell, V. Cirigliano, M. J. Ramsey-Musolf, P. Vogel and M. B. Wise, *How magnetic is the Dirac neutrino?*, *Phys. Rev. Lett.* **95** (2005) 151802 [hep-ph/0504134].

- [44] T. Han, J. Liao, H. Liu and D. Marfatia, *Scalar and tensor neutrino interactions*, 2004.13869.
- [45] T. Hahn, *Generating Feynman diagrams and amplitudes with FeynArts 3*, *Comput. Phys. Commun.* **140** (2001) 418 [hep-ph/0012260].
- [46] T. Hahn and M. Perez-Victoria, *Automatized one loop calculations in four-dimensions and D-dimensions*, *Comput. Phys. Commun.* **118** (1999) 153 [hep-ph/9807565].
- [47] G. Buchalla, A. Celis, C. Krause and J.-N. Toelstede, *Master Formula for One-Loop Renormalization of Bosonic SMEFT Operators*, 1904.07840.
- [48] F. Takahashi, M. Yamada and W. Yin, *XENON1T anomaly from anomaly-free ALP dark matter and its implications for stellar cooling anomaly*, 2006.10035.
- [49] K. Kannike, M. Raidal, H. Veermäe, A. Strumia and D. Teresi, *Dark Matter and the XENON1T electron recoil excess*, 2006.10735.
- [50] G. Alonso-Álvarez, F. Ertas, J. Jaeckel, F. Kahlhoefer and L. Thormaehlen, *Hidden Photon Dark Matter in the Light of XENON1T and Stellar Cooling*, 2006.11243.
- [51] B. Fornal, P. Sandick, J. Shu, M. Su and Y. Zhao, *Boosted Dark Matter Interpretation of the XENON1T Excess*, 2006.11264.
- [52] C. Boehm, D. G. Cerdeno, M. Fairbairn, P. A. Machado and A. C. Vincent, *Light new physics in XENON1T*, 2006.11250.
- [53] K. Harigaya, Y. Nakai and M. Suzuki, *Inelastic Dark Matter Electron Scattering and the XENON1T Excess*, 2006.11938.
- [54] A. Bally, S. Jana and A. Trautner, *Neutrino self-interactions and XENON1T electron recoil excess*, 2006.11919.
- [55] L. Su, W. Wang, L. Wu, J. M. Yang and B. Zhu, *Xenon1T anomaly: Inelastic Cosmic Ray Boosted Dark Matter*, 2006.11837.
- [56] M. Du, J. Liang, Z. Liu, V. Q. Tran and Y. Xue, *On-shell mediator dark matter models and the Xenon1T anomaly*, 2006.11949.
- [57] L. Di Luzio, M. Fedele, M. Giannotti, F. Mescia and E. Nardi, *Solar axions cannot explain the XENON1T excess*, 2006.12487.
- [58] U. K. Dey, T. N. Maity and T. S. Ray, *Prospects of Migdal Effect in the Explanation of XENON1T Electron Recoil Excess*, 2006.12529.

- [59] N. F. Bell, J. B. Dent, B. Dutta, S. Ghosh, J. Kumar and J. L. Newstead, *Explaining the XENON1T excess with Luminous Dark Matter*, 2006.12461.
- [60] Y. Chen, J. Shu, X. Xue, G. Yuan and Q. Yuan, *Sun Heated MeV-scale Dark Matter and the XENON1T Electron Recoil Excess*, 2006.12447.
- [61] D. Aristizabal Sierra, V. De Romeri, L. Flores and D. Papoulias, *Light vector mediators facing XENON1T data*, 2006.12457.
- [62] J. Buch, M. A. Buen-Abad, J. Fan and J. S. C. Leung, *Galactic Origin of Relativistic Bosons and XENON1T Excess*, 2006.12488.
- [63] G. Choi, M. Suzuki and T. T. Yanagida, *XENON1T Anomaly and its Implication for Decaying Warm Dark Matter*, 2006.12348.
- [64] G. Paz, A. A. Petrov, M. Tamaro and J. Zupan, *Shining dark matter in Xenon1T*, 2006.12462.
- [65] H. M. Lee, *Exothermic Dark Matter for XENON1T Excess*, 2006.13183.
- [66] R. Primulando, J. Julio and P. Uttayarat, *Collider Constraints on a Dark Matter Interpretation of the XENON1T Excess*, 2006.13161.
- [67] K. Nakayama and Y. Tang, *Gravitational Production of Hidden Photon Dark Matter in light of the XENON1T Excess*, 2006.13159.
- [68] Y. Jho, J.-C. Park, S. C. Park and P.-Y. Tseng, *Gauged Lepton Number and Cosmic-ray Boosted Dark Matter for the XENON1T Excess*, 2006.13910.
- [69] M. Baryakhtar, A. Berlin, H. Liu and N. Weiner, *Electromagnetic Signals of Inelastic Dark Matter Scattering*, 2006.13918.
- [70] H. An, M. Pospelov, J. Pradler and A. Ritz, *New limits on dark photons from solar emission and keV scale dark matter*, 2006.13929.
- [71] A. E. Robinson, *XENON1T observes tritium*, 2006.13278.
- [72] A. N. Khan, *Can nonstandard neutrino interactions explain the XENON1T spectral excess?*, 2006.12887.
- [73] C. Giunti and A. Studenikin, *Neutrino electromagnetic interactions: a window to new physics*, *Rev. Mod. Phys.* **87** (2015) 531 [1403.6344].
- [74] PARTICLE DATA GROUP collaboration, *Review of Particle Physics*, *Phys. Rev.* **D98** (2018) 030001.

- [75] A. Ishikawa, *Search for invisible decays of the Higgs boson at the ILC*, *PoS LeptonPhoton2019* (2019) 147 [1909.07537].
- [76] A. Alloul, N. D. Christensen, C. Degrande, C. Duhr and B. Fuks, *FeynRules 2.0 - A complete toolbox for tree-level phenomenology*, *Comput. Phys. Commun.* **185** (2014) 2250 [1310.1921].
- [77] P. Nogueira, *Automatic Feynman graph generation*, *J. Comput. Phys.* **105** (1993) 279.